Available online at www.sciencedirect.com

SciVerse ScienceDirect

journal homepage: www.elsevier.com/locate/issn/15375110

Research Paper

Modelling and simulation of cross flow grain dryers

O.A. Khatchatourian [a,*], H.A. Vielmo [b], L.A. Bortolaia [a]

[a] Department of Exact Sciences and Engineering, Regional University of the Northwest, Rio Grande do Sul, R. São Francisco, 501, 98700-000, Ijuí, RS, Brazil

[b] Department of Mechanical Engineering, Federal University of Rio Grande do Sul, Rua Sarmento Leite, 425, 90050-170, Porto Alegre, RS, Brazil

ARTICLE INFO

Article history:
Received 26 January 2013
Received in revised form
23 August 2013
Accepted 2 September 2013
Published online 12 October 2013

A mathematical model, algorithm, and computer program were developed to simulate the performance of cross flow grain dryers and cross flow dryers with energy saving. The mass and heat transfer processes were described by a system of four non-linear partial differential equations. This system of equations was solved by the MacCormack method with time splitting. The Neumann method was used to determine convergence. The source-terms in these equations were computed by auxiliary semi-empirical equations obtained by experimental data from thin layer drying. Equipment developed to obtain these data permitted variation of the initial air humidity, temperature, and velocity. Fixed bed drying experiments were conducted to validate the model. Simulations using various control regimens were made to determine the impact on energy consumption and cross flow dryer performance due to recycling air exhausted from various stages of the dryer. An iterative process was used to determine the initial conditions at the entrance to each section of the dryer. The computer simulations were used to evaluate the non-uniformity of temperature and grain moisture content distributions in dryers, the duration of the drying process and the energy efficiency for each geometry and control regimen.

1. Introduction

Due to the humid climate that occurs during the soya bean harvest, the moisture content of seed may be as high as 24–28% dry basis, (d.b.). Therefore practically all soya beans must be thermally dried before storage. Considering the amount harvested, even minor improvements and accelerations in the drying process will provide significant economic benefit.

Mathematical modelling and computer simulation are widely used to design dryers and develop efficient grain drying control systems (Courtois, Lebert, Lasseran, & Bimbenet, 1991; França, Fortes, & Haghighi, 1994; Han, Zuo, Zhu, Wu, & Liu, 2012; Liu & Bakker-Arkema, 2001). There are various mathematical models to describe the drying process. These models consider the heat and mass transfer between grain and air, the heat and moisture transfer inside the grain, deviations from the equilibrium state between the grain and drying air, and variations in the physical properties of air, water vapour, and grains due to variations in temperature and humidity (Barrozo, Felipe, Sartori, & Freire, 2006; Barrozo, Henrique, Sartori, & Freire, 1999; Brooker, Bakker-Arkema, & Hall, 1982; Luikov, 1966; Parry, 1985).

Generally these models represent a system of differential equations describing the energy and moisture transfer for an individual grain located in a layer, at the grain surface, and the

* Corresponding author.
E-mail address: olegkha@unijui.edu.br (O.A. Khatchatourian).
1537-5110/$ – see front matter © 2013 IAgrE. Published by Elsevier Ltd. All rights reserved.
http://dx.doi.org/10.1016/j.biosystemseng.2013.09.001

Nomenclature

a	grain surface area/volume ratio, m^{-1}
A	binary matrix
A_i	lateral area of the air inlet, m^2
C_{pg}	specific heat of the grain, J kg^{-1} K^{-1}
C_{pv}	specific heat of the water's vapour, J kg^{-1} K^{-1}
C_{pw}	specific heat of the water, J kg^{-1} K^{-1}
F	column of the right sides
H_v	latent heat of the water vaporization, J kg^{-1};
k_1, k_2	proportionality coefficients,
L	bed height, column width, m
L_x, L_y	MacCormack's operators
M	grain moisture content, decimal, d.b.
n	quantity of stages or constant
q	velocity factor, dimensionless
t	time, s
T_a	air temperature, °C
T_g	grain temperature, °C
T_i	initial air temperature to stage i
U	column-vector of the unknown functions
V_x	horizontal air velocity, m s^{-1}
V_y	grain velocity, m s^{-1}
W	air humidity, decimal
ε	porosity, dimensionless
ρ_a	specific mass of the air, kg m^{-3}
ρ_g	specific mass of the grain, kg m^{-3}
Φ_h	heat flux, W m^{-2}
Φ_m	mass flux, kg m^{-2} s^{-1}

Subscripts:

0	initial
1	first stage
2	second stage
a	air
c	cooling
e	equilibrium
g	grain
i	stage order number,

conservation of energy and mass at the boundary layer between the grain and humid air (Brooker et al., 1982; Khatchatourian & Oliveira, 2006). The nonlinearity of these equations does not allow for an analytical solution. The numerical methods used (finite difference method, finite element method, etc.) represent the integration domain (the drying chamber) as a set of subdomains in which any parameter, at any moment in time, is found by using simplified interpolation equations (usually linear or square-law). Since the size of the spatial elements is small, and the time step is small, the change in the parameters within a single element is insignificant; therefore to calculate the local mass flow and heat flow densities a thin-layer drying model can be used (Jayas, Cenkowski, Pabis, & Muir, 1991; Parti, 1993). Thus, the quality of thin-layer drying models essentially defines the simulation results for bulk drying.

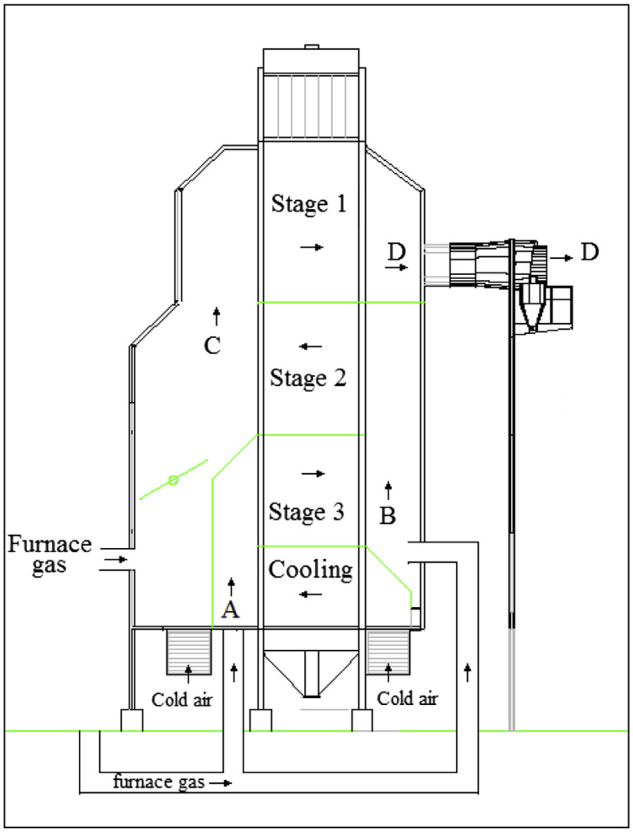

Fig. 1 – Layout of continuous flow grain dryer with three drying stages and cooling chamber.

This paper is dedicated to modelling of cross flow grain dryers (Fig. 1) widely used for drying of soya beans in the Rio Grande do Sul State, Brazil.

Cross flow grain dryers have been studied by several authors, for example, Barrozo, Felipe, Sartori, and Freire (2006), Eltigani and Bakker-Arkema (1987), Giner, Mascheroni, and Nellist (1996), Han et al. (2012), Mayta, Massarani, and Pinto (1996), Liu and Bakker-Arkema (2001), Moreira and Bakker-Arkema (1990), Platt, Rumsey, and Palazoglu (1991), Rumsey and Rovedo (2001), Tórrez, Gustafsson, Schreil, and Martínez (1998), Zhihuai and Chongwen (1999). Models used in earlier studies were presented in summary form in Laws and Parry (1983), and described in review by Parry (1985). However, to select the optimal scheme and parameters of cross flow grain dryers further investigation is required. Except for general recommendations based on the experiences and preferences of some authors (for example, Kemp, 1999; Marinos-Kouris, Maroulis, & Kiranoudis, 1998; Rumsey & Rovedo, 2001, etc.), no systematic studies on the selection of the optimal number of drying steps, the initial temperature distribution for each stage, the ratio of heights between the stages, the analysis of non-uniformity of temperature and moisture concentration, the impact of recirculating exhaust air from the drying zones into the previous chamber, occur in the literature. In particular, the calculation of the effect of recirculating exhaust air requires knowledge of the effect of increased initial air humidity on grain drying, and the authors have dedicated a lot of effort to study this effect (Khatchatourian, 2012).

The principal objectives of the present work were to:

a) create a mathematical model of drying of grains;
b) develop software for simulation of continuous cross flow dryer with multiple stages;
c) carry out simulations to evaluate the efficiency of various dryer control schemes.

2. Mathematical model

Figure 1 represents one of the continuous flow grain dryers investigated. It has three drying stages and one cooling chamber. Ambient air passes through the cooling chamber, it is then heated as it passed through the warm grain and is mixed with the heated furnace air. This mixture *A* passes through the grain in the third stage. Air leaving the third stage, mixes with the heated furnace air and the resulting mixture *B* enters in the second stage. Similarly, the mixture *C* enters in the first stage, heats up and dries the grain entering from above and used air is then exhausted to the atmosphere.

In summary, the cross flow drying model for these conditions is:

$$\begin{cases} \frac{\partial T_a}{\partial t} + V_x\frac{\partial T_a}{\partial x} + V_y\frac{\partial T_a}{\partial y} = -\frac{a(1-\varepsilon)}{\rho_a\ \varepsilon}\cdot\frac{\Phi_m C_{pv}\left(T_g - T_a\right)+\Phi_h}{C_{pa}+C_{pv}W} \\ \frac{\partial T_g}{\partial t} = \frac{a\left\{\Phi_h - \Phi_m\left[H_v + \left(C_{pv}-C_{pw}\right)T_g\right]\right\}}{\rho_g\left(C_{pg}+MC_{pw}\right)} \\ \frac{\partial W}{\partial t} + V_x\frac{\partial W}{\partial x} + V_y\frac{\partial W}{\partial y} = \frac{\Phi_m a\ (1-\varepsilon)}{\rho_a \varepsilon} \\ \frac{\partial M}{\partial t} = -\frac{\Phi_m a}{\rho_g} \end{cases} \quad (1)$$

where M is the grain moisture content, d.b.; W is the air humidity; a is grain surface area/volume ratio in m^{-1}; H_v is latent heat of the water vaporization in J kg^{-1}; C_{pg} is the specific heat of the grain in J kg^{-1} K^{-1}; C_{pv} is the specific heat of the water vapour in J kg^{-1} K^{-1}; C_{pw} is the specific heat of the water in J kg^{-1} K^{-1}; ρ_g is the specific mass of the grain in kg m^{-3}; ρ_a is specific mass of the air in kg m^{-3}; ε is porosity; V_x is the air velocity in m s^{-1}; V_y is the vertical velocity in m s^{-1}; T_a is the air temperature in °C; T_g is the grain temperature in °C; Φ_h is the heat flux in W m^{-2}; Φ_m is the mass flux in kg m^{-2} s^{-1}.

Since the vertical component of the velocity is small relative to the velocities in the horizontal directions, the structure of the grain mass in a cross flow dryer is similar to the structure in a fixed-bed dryer. Therefore, it is not correct to take into account the convective term caused by the grain mass movement for cross-flow drying model, as suggested in some works (for example, in Parry, 1985; Rumsey, 1986; Rumsey & Rovedo, 2001).

The system of equations is obtained by means of the Lagrangian specification of the flow field and has some differences from the system of equations proposed in Brooker et al. (1982). For example, the terms, related with the vapour heating from T_g to T_a, are included in the energy equation for the gas, but not for grain. In the equation for the enthalpy change of grain there is enthalpy of water that leaves the grain and then evaporates into the gas phase. There are also some partial derivatives for the parameters of moist air which were neglected by Brooker et al. (1982).

The heat flux, Φ_h, was calculated in accordance using the relationships, presented by Khatchatourian and Oliveira (2006). As their experimental study showed, the diffusion coefficient for soya bean seed has a variable value in a radial direction. Therefore, in this work, to determine the mass flux Φ_m, a two-compartment grain model for soya bean thin-layer drying was chosen. The mathematical model was presented by a system of two ordinary differential equations (Khatchatourian, 2012):

$$\begin{cases} \frac{dM_1}{dt} = -k_1(M_1 - M_2); \\ \frac{dM_2}{dt} = -k_1(M_2 - M_1) - q\cdot k_2\left(M_{g0} - M_e\right)^{n-1}M_2^n \end{cases} \quad (2)$$

where M_1 and M_2 are average relative moisture content of grain in the first and the second grain compartments respectively, k_1 and k_2 are proportionality coefficients, t is time in s, n is constant, q is a factor related with velocity influence.

The coefficient, k_1, is related with a diffusion coefficient in the first compartment and k_2 unites the effects of diffusion in the second compartment and convective transfer at the grain surface.

The second equation in the system Eq. (2) represents the influence of the initial grain moisture content (M_0) and the air humidity through equilibrium moisture content (M_e) on the drying rate. Applying the inverse problem method, the coefficients k_1 and k_2 were obtained for different initial grain moisture contents and temperatures at the same velocity V_x = 0.9 m s^{-1} (q = 1). As experimental data show (Khatchatourian, 2012) the coefficients k_1 and k_2 depend on temperature. The influence of initial grain moisture content on k_1 and k_2 can be neglected. To take into account the influence of velocity on drying, the coefficient k_2 was multiplied by a factor:

$$q = 1.25 - 1.1e^{-1.52V^{0.048+1.21M_0}} \quad (3)$$

The factor is equal to 1 when V_x = 0.9 m s^{-1} (basic velocity) and M_0 = 0.16.

The initial and boundary conditions for grain mass in each stage depend on the parameters in the output of the previous stage located immediately above. Furthermore, the inlet air humidity (boundary condition for air humidity) depends on the amount of air recirculation. In other words, these conditions depend on the number of stages and the scheme of distribution and recirculation of air.

Figure 2 shows some schemes of dryers which were considered in this work.

For Scheme 3 (Fig. 2), which corresponds to the layout of a cross flow grain dryer with three drying stages (Fig. 1), the initial and boundary conditions for stage i were described as follows:

The boundary conditions:

$$M_1(t,x,0) = M_0; T_{g1}(t,x,0) = T_{g0}; T_1(t,0,y) = T_{a1}; T_2(t,0,y) = T_{a2}; T_3(t,0,y) = T_{a3}.$$

The boundary conditions for variables $M_2(t, x, H_1)$, $T_2(t, x, H_1)$, $M_3(t, x, H_1 + H_2)$, $T_{g3}(t, x, H_1 + H_2)$, $M_c(t, x, H_1 + H_2 + H_3)$, $T_{gc}(t, x, H_1 + H_2 + H_3)$, W_1, W_2, W_3 were determined during the calculations by iterative process.

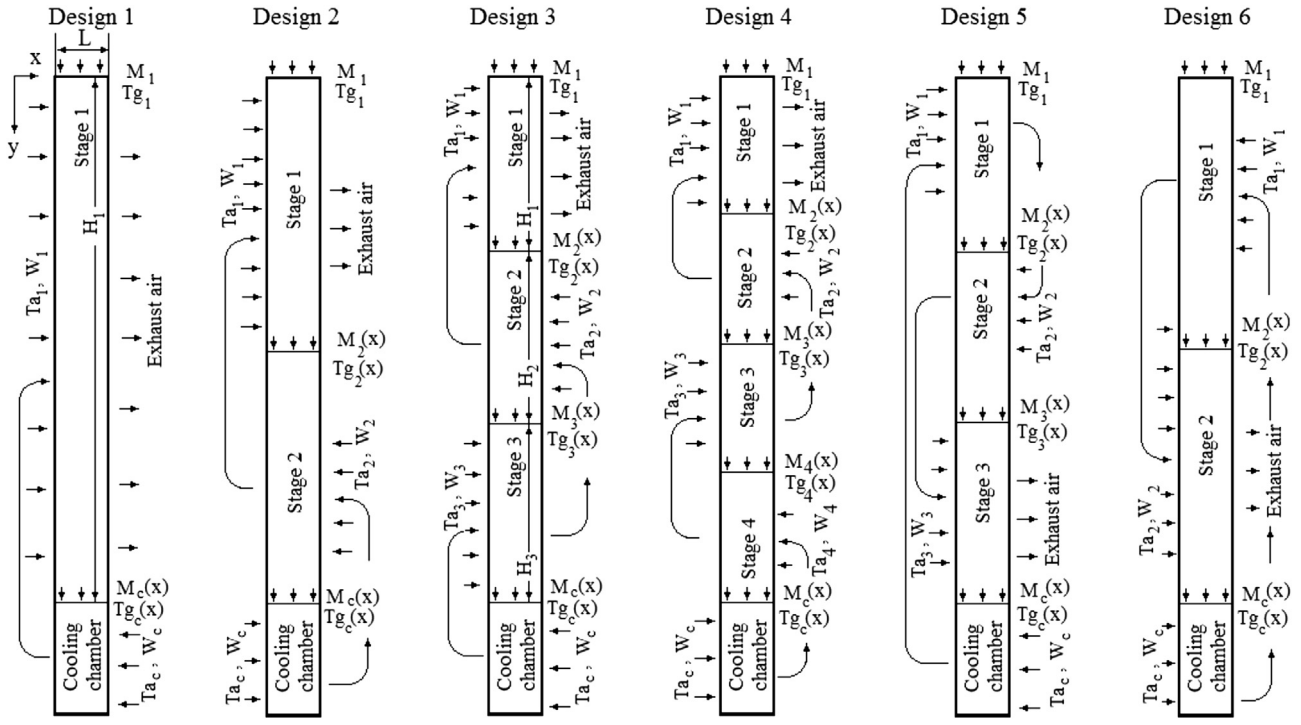

Fig. 2 – Investigated dryer outline designs.

The initial conditions:

$$M_i(0,x,y) = M_0; T_{gi}(0,x,y) = T_{g0}; W_i(0,x,y) = W_0; T_{ai}(0,x,y) = T_{g0}(i = 1,2,3,c),$$

where the indices *a*, *g*, *c* correspond to air, grain and the cooling chamber respectively.

3. Solution of the partial differential equations

The system (hyperbolic) of partial differential quasi-linear equations was rewritten in the matrix form:

$$\frac{\partial U}{\partial t} + A \cdot \left[\frac{\partial U}{\partial x} \; \frac{\partial U}{\partial y}\right] \begin{pmatrix} V_x \\ V_y \end{pmatrix} = F(t,x,y,U) \tag{4}$$

where U is the column-vector of the unknown functions; A is the binary matrix; F is the column of the right sides of the system (1):

$$U = \begin{pmatrix} T_a \\ T_g \\ W \\ M \end{pmatrix}; \quad A = \begin{bmatrix} 1 & 0 & 0 & 0 \\ 0 & 0 & 0 & 0 \\ 0 & 0 & 1 & 0 \\ 0 & 0 & 0 & 0 \end{bmatrix}; \quad F = \begin{pmatrix} F_1 \\ F_2 \\ F_3 \\ F_4 \end{pmatrix}. \tag{5}$$

To solve the system, a two-dimensional MacCormack's method with scheme "time-split" (MacCormack, 1971; MacCormack & Paullay, 1972) was used.

The iterative MacCormack's method with the "time-split" transforms the two-dimensional problem in sequence of one-dimensional problems. Considering the differential operator L_x, related to the spatial variable x:

$$U^*_{i,j} = L_x(\Delta t_x) U^n_{i,j} \tag{6}$$

The MacCormack's method (MacCormack, 1969) corresponds to the sequence of operations:

Predictor:

$$\overline{U^*_{i,j}} = U^n_{i,j} - \frac{\Delta t_x \cdot V_x}{\Delta x}\left[U^n_{i+1,j} - U^n_{i,j}\right] + \Delta t_x F^n_{i,j} \tag{7}$$

Corrector:

$$U^*_{i,j} = \frac{1}{2}\left[U^n_{i,j} + \overline{U^*_{i,j}} - \frac{\Delta t_x \cdot V_x}{\Delta x}\left(\overline{U^*_{i,j}} - \overline{U^*_{i-1,j}}\right)\right] + \frac{\Delta t_x \overline{F^*_{i,j}}}{2} \tag{8}$$

The asterisk (*) is used to denote the parameters with intermediate time steps. The equations for the variables T_g and X_g don't contain the terms with the velocities.

L_y operator was defined similarly substituting V_x and t_x by V_y and t_y. The MacCormack's method with the "time-split" can be presented as:

$$U^{n+1}_{i,j} = L_x\left(\frac{\Delta t_x}{2}\right) L_y(\Delta t_y) L_x\left(\frac{\Delta t_x}{2}\right) U^n_{i,j} \tag{9}$$

Assuming V_x and V_y as constants, the operator L_x for the half time-step and the derivatives with respect to x, is composed of:

Predictor:

$$\overline{U^{*n+1/2}_{i,j}} = U^n_{i,j} - \frac{\Delta t_x V_x}{2\Delta x}\left[U^n_{i+1,j} - U^n_{i,j}\right] + \frac{\Delta t_x}{2} F^n_{i,j} \tag{10}$$

Corrector:

$$U_{i,j}^{*n+1/2} = \frac{1}{2}\left[U_{i,j}^{n} + \overline{U_{i,j}^{*n+1/2}} - \frac{\Delta t_x V_x}{2\Delta x}\left(\overline{U_{i,j}^{*n+1/2}} - \overline{U_{i-1,j}^{*n+1/2}}\right)\right] + \frac{\Delta t_x \overline{F_{i,j}^{*n+1/2}}}{2} \quad (11)$$

The operator L_y for full time step and the derivatives with respect to y is formed:

Predictor:

$$\overline{U_{i,j}^{**}} = U_{i,j}^{*n+1/2} - \frac{\Delta t_y V_y}{\Delta y}\left[U_{i,j+1}^{*n+1/2} - U_{i,j}^{*n+1/2}\right] + \Delta t_y F_{i,j}^{*n+1/2} \quad (12)$$

Corrector:

$$U_{i,j}^{**} = \frac{1}{2}\left[U_{i,j}^{*n+1/2} + \overline{U_{i,j}^{**}} - \frac{\Delta t_y V_y}{\Delta y}\left(\overline{U_{i,j}^{**}} - \overline{U_{i,j-1}^{**}}\right)\right] + \Delta t_y \overline{F_{i,j}^{**}} \quad (13)$$

And again the operator L_x:

Predictor:

$$\overline{U_{i,j}^{n+1/2}} = U_{i,j}^{**} - \frac{\Delta t_x V_x}{2\Delta x}\left[U_{i+1,j}^{**} - U_{i,j}^{**}\right] + \frac{\Delta t_x}{2} F_{i,j}^{**} \quad (14)$$

Corrector:

$$U_{i,j}^{n+1} = \frac{1}{2}\left[U_{i,j}^{**} + \overline{U_{i,j}^{n+1/2}} - \frac{\Delta t_x V_x}{2\Delta x}\left(\overline{U_{i,j}^{n+1/2}} - \overline{U_{i-1,j}^{n+1/2}}\right)\right] + \frac{\Delta t_x \overline{F_{i,j}^{n+1/2}}}{2} \quad (15)$$

The software was developed in Dev-Pascal 1.9.2 (distributed under the GNU General Public License, http://www.bloodshed.net/devpascal.html) and consists of tools for geometry construction and mesh generation. Three iterative processes were used for simulation: a) the first (internal) was used for each time step to compute the source terms (due to their non-linearity); b) the second (intermediate) was used to determine the boundary conditions between stages and air humidity in the side entrance to each stage (which depends on the composition of the air furnace + fresh air + air recirculation); c) the third iterative process (external) was applied to calculate the drying time to achieve the required average moisture content of grain in the dryer outlet (15% d.b.), *i.e.*, to calculate the vertical velocity V_y. The stability analysis was realised using the Neumann method; the time steps Δt_x, Δt_y and the length intervals Δx, Δy were chosen to satisfy the Courant–Friedrichs–Lewy condition (Courant, Friedrichs, & Lewy, 1967).

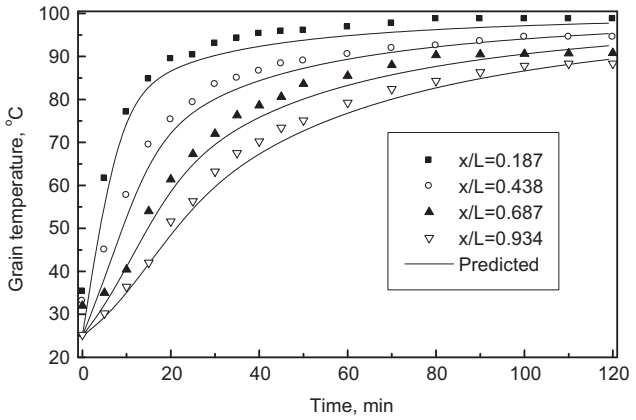

Fig. 4 – Comparison between experimental and predicted grain temperatures in different sections of drying chamber.

4. Validation of the developed model

To validate the developed model, experiments on the drying dynamics of soya beans in a fixed bed were conducted and the comparisons were made between values obtained experimentally and by the simulations. Figure 3 shows the experimental equipment used to study the drying dynamics in the fixed bed. The equipment consists of a ventilating fan, orifice plate, heat booster, steam generation and injection systems, a data acquisition system, and the drying chamber. The drying

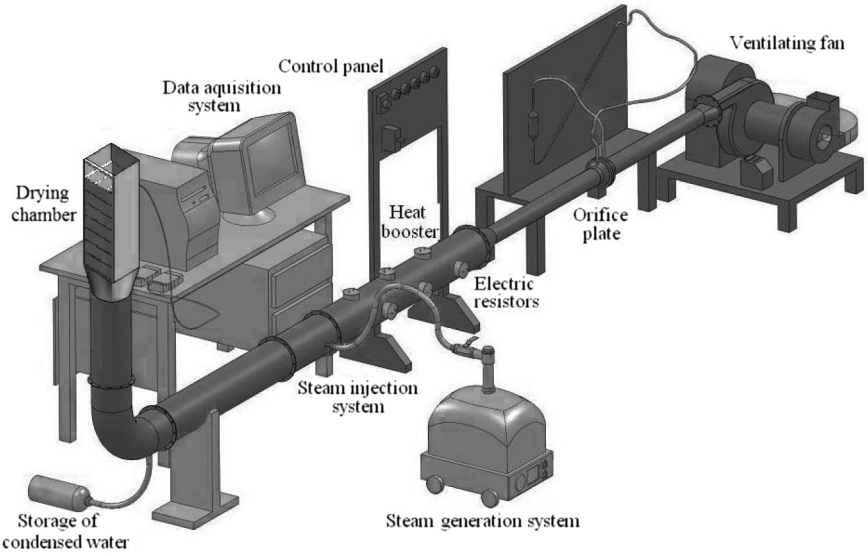

Fig. 3 – Experimental equipment.

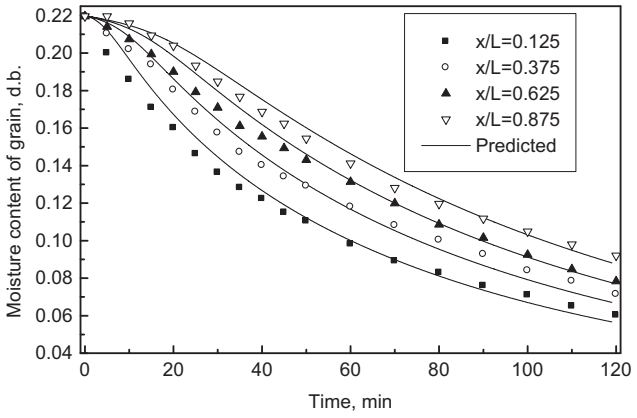

Fig. 5 – Experimental and predicted dynamics of soya beans drying in fixed bed.

tests were conducted for soya bean in the temperature range 70–110 °C and velocity range 0.2–0.9 m s^{-1}. The drying chamber consisted of seven sections, each measuring 0.05 × 0.13 × 0.13 m with total height of 0.35 m. Each section has a height of 0.05 m; the chamber was insulated with glass wool.

Each section was removable and had a perforated screen on the bottom. The experiments were conducted using four sections of the drying chamber, resulting a bed height of 0.2 m. Temperatures of air and grain were measured in all four sections by Type-K thermocouples with precision ±0.75%. Using a digital analytical balance with 0.001 g readability, the dynamics of grain mass loss in each section was determined, allowing the determination of the variation of moisture content of grain. The air temperature was measured at the outlet of each section. The grain temperature was measured by placing a Type-K thermocouple junction at the centre of an individual seed located 0.01 m from the outlet of each section. Soya beans for the experiments were stored with a moisture content of 22% (d.b.). Each experiment was repeated 3–4 times with the same initial conditions.

The comparison between the experimental data for soya beans (T_a = 100 °C; V_x = 0.5 m s^{-1}) and simulation results for the fixed bed are shown in Figs. 4–6. Figure 4 shows the dynamics of variation of the grain temperature along the measuring chamber. The layers that are closer to the input section, heated much faster than the layers at the exit of the chamber. Accordingly, the drying process (Fig. 5) was non-uniform with the layers near the air inlet (x/H = 0.25) drying faster. Layers at the exit of the chamber (x/H = 1.0) dried more slowly. The variation of the calculated and measured air temperature in the drying process is shown in Fig. 6.

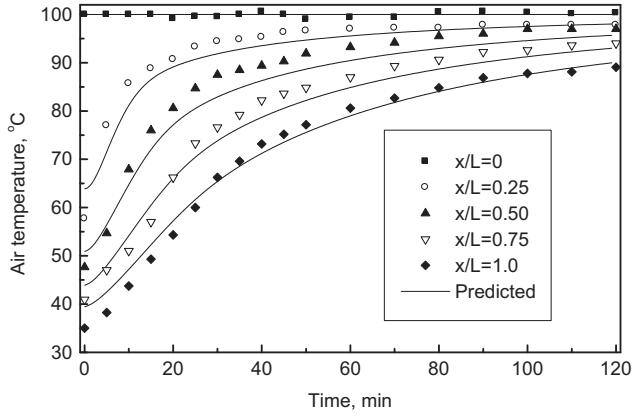

Fig. 6 – Comparison between experimental and predicted air temperatures in different sections of drying chamber.

Comparative analysis of the calculated and experimental results shows that the developed model adequately described the processes involved in the drying process. There was a small tendency for a lag in time between the predicted and experimental data which can be neglected since calculations of drying in this case will guarantee that the required grain moisture is achieved at the selected drying time.

Figure 7 shows a significant variation in humidity in the fixed bed. Air humidity reaches a maximum after 10–20 min of drying, that undoubtedly affects the local process of drying and therefore the influence of air humidity should be considered in the calculations.

5. Simulation of results

Using the developed model, various numerical simulations were made. Initially, the influence of airflow direction reversals along the height of the dryer on the non-uniformity of grain temperature and moisture content distributions was studied. Subsequently the influence of air humidity increase caused by reuse of drying air on the drying dynamics and drying time was studied.

5.1. *Influence of number of airflow direction reversals*

Various dryers with the same overall column height (10.47 m) composed of the several equal drying stages were compared (Fig. 2 shows the first six schemes with drying stages numbered from 1 to 4). Each a dryer had a 2.13 m height cooling chamber. For each subsequent stage there was a consecutive reversal of the airflow direction. The initial temperatures for all stages were set to 100 °C.

The distribution of the grain moisture content in outlet cross-section of studied dryers (curves number corresponds to dryers order number in Table 1) is non-uniform and this non-uniformity depends strongly on the dryer outline (Fig. 8).

Figure 9 shows the influence of stage number on distribution non-uniformity of grain moisture content and grain temperature in outlet cross-section of dryer (at the cooling inlet). A non-uniformity was estimated by means of the maximum relative difference of grain temperature $\delta T_{max} = (T_{max} - T_{min})/T_{mean}\cdot 100\%$ and moisture content $\delta M_{max} = (M_{max} - M_{min})/M_{mean}\cdot 100\%$ in considered section (square points), or by mean-square deviation from the mean in the horizontal direction $\delta T = \sqrt{\int_0^1 (T - T_{mean})^2 dx}/T_{mean}\cdot 100\%$ and $\delta M = \sqrt{\int_0^1 (M - M_{mean})^2 dx}/M_{mean}\cdot 100\%$ (triangular points). As it was expected, the airflow direction reversal reduces the

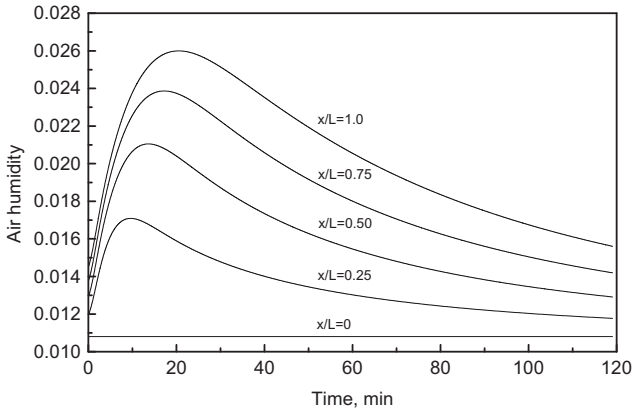

Fig. 7 – Predicted dynamics of air humidity variation in different sections of drying chamber.

non-uniformity of all parameters in outlet cross-section of dryer.

There is a general tendency for the non-uniformity of temperature and grain moisture content distributions in outlet cross-section of dryer to decrease as the number of stages increases. These relationships have local minima (for even values of the number of stages), and the local maxima (for odd values).

This is a consequence of the fact that for an even number of stages there are the same inlet conditions of the drying air to both sides of the column.

The minimum of the moisture content non-uniformity, achieved with two stages, is a global, and the increase in the number of stages (>4) does not improve the uniformity of the field. As the calculations show (Fig. 10), the drying time is slightly increased with the number of stages (triangular points). Probably, an equalisation of temperature field results in the reduction of grain quantity subjected to higher temperature, when the drying process is most intensive. In return with increasing number of stages the possibility of heat regeneration (square points) increases significantly.

It can be concluded that among the considered dryers, the scheme with two stages is the most acceptable. With a relatively small increase in drying time, this scheme presents the output parameters field with the least non-uniformity, and the possibility for energy saving is high (up to 34%). To regenerate the heat, the air, heated by contact with hot grain in previous stages, was mixed, with furnace air at 300 °C. Air velocity in each stage was equal. Air humidity at the inlet to each stage depended on the fraction and humidity of the reuse air.

5.2. *Influence of air humidity increase caused by reuse of drying air*

Figure 11 shows the effect of additional humidity caused by air reused, on the drying process in a dryer with four stages. This effect is significant for last layers of the upper stage (stage 1). When the grain moves down, this influence diminishes and becomes negligible near the exit section of the dryer. Calculations show that the drying time for the dryer with four stages is increased by less than 1% in the case of air reuse by increasing the air humidity at the inlet to each stage. At the same time the heat recovery under these conditions can reach 45% (Fig. 10).

Subsequently, the influence of the initial temperature distribution in the air inlet of each stage was studied. To equalise the consumption of energy per unit of time for each studied scheme the sum of the products of initial temperature on the lateral area of stage was kept constant, *i.e.*: $\sum_{i=1}^{n} T_i A_i = \text{constant}$, where T_i is the initial temperature of the air to stage i, A_i is the lateral area of the air inlet, i is the stage order number, n is the quantity of stages.

Table 1 shows the initial temperatures of the air for the studied dryers, their non-uniformity characteristics, energy saving and relative drying time.

It is interesting to note that both the maximum relative difference between the parameters and the standard deviation from the mean can be used for comparison to non-uniformity of the dryer, because the correlation coefficient between them is greater than 0.995. Comparative analysis of the effectiveness of these dryers can be made using Fig. 12, which shows a total non-uniformity of the temperature and concentration fields. Lowering the temperature of the stages that are close to the cooling reduces the non-uniformity of the temperature field (dryers 4, 9 and 11). Increasing the length of continuous domains with high temperature reduces the non-uniformity of the moisture content field (dryers 2, 5, 6, 8, 10 and 11). Despite the fact that concentration non-uniformity is minimal for the dryer 2 (two stages with the same inlet temperature), the lowest total non-uniformity is achieved for the dryer 8 (three stages with temperatures 100–120–80 °C, respectively), the second lowest is for dryer 6, and the third for dryer 2.

Simulation results of dryer 6 are shown in Figs. 13–16. The values of the parameters were taken as follows: $H_1 = H_2 = H_3 = 3.49$ m; $L = 0.167$ m; air velocity $V_x = 0.4$ m s^{-1}; $M_0 = 0.22$ (d.b.); $T_{g0} = 20$ °C; $T_{a1} = 120$ °C; $T_{a2} = 100$ °C; $T_{a3} = 80$ °C; $T_{ac} = 25$ °C.

It can be seen in Fig. 13 that the drying process in the initial ($x/L = 0$) and final ($x/L = 1$) sections occurs the most rapidly. In the middle section ($x/L = 0.5$) drying curve lags behind the average. Air and grain temperatures in the different cross-sections (Figs. 14 and 15) differ significantly in only the first stage. For subsequent stages the temperature difference decreases.

Air humidity at the outlet of the first stage varies significantly with height (Fig. 16). For subsequent stages this difference is not very large. The highest moisture air for drying enters the first stage, because this air contains all the moisture received from the grain in second and third stages. As the air temperature at the inlet of the cooling chamber was chosen relatively low ($T_a = 25$ °C), the variations in grain moisture and air humidity inside the cooling chamber were not great. This allows monitoring of the completeness of the drying process in any section of the cooling chamber.

Comparative analysis of the calculations made for Schemes 3 and 5 (from Fig. 2) with $T_{a1} = 120$ °C; $T_{a2} = 100$ °C; $T_{a3} = 80$ °C; $T_{ac} = 25$ °C, shows that Scheme 3 results in a large reduction in energy (Fig. 18, solid points) despite the fact that

Table 1 – Simulation details of studied dryers: number of stages, initial temperatures of the air, non-uniformity characteristics, energy saving and relative drying time.

Simulation number	1	2	3	4	5	6	7	8	9	10	11
Number of stages	1	2	2	2	3	3	3	3	3	3	3
Initial temperature, °C	100	100	120	80	100	120	120	100	100	80	80
		100	80	120	100	100	80	120	80	120	100
					100	80	100	80	120	100	120
δT_{max}, %	38.3	33.3	17.7	49.3	34.3	19.8	38.9	16.3	52.4	31.7	49.2
δM_{max}, %	39.5	15.0	31.8	24.8	19.0	23.2	31.8	19.6	30.6	19.6	20.9
δT, %	11.3	10.1	5.2	15.3	11.0	6.5	12.4	5.3	16.7	10.1	15.7
δM, %	11.4	4.0	9.4	7.0	5.2	6.1	9.2	5.1	9.1	5.0	5.9
Energy saving, %	7.45	33.6	30.3	34.8	41.0	39.7	39.9	40.3	40.2	40.8	40.7
Relative drying time	1.00	1.05	1.07	1.02	1.09	1.09	1.10	1.08	1.08	1.07	1.06

the average percentage of recycled air is greater for Scheme 5 (Fig. 18, open points). This is due to the fact that the used air, exhausted from the third stage and having a higher average temperature than exhausted from the first stage, in Scheme 5 is exhausted to the atmosphere, but in Scheme 3 it is applied for reuse. In addition, there is a small increase of the drying time for Scheme 5 (between 2 and 3%). This increase is related to the influence of the initial air humidity at the inlet to each stage. A comparison between Figs. 16 and 17 shows that air humidity at the entrance to the stages 2 and 1 (Scheme 3) is less than for the corresponding stages 2 and 3 of Scheme 5. Similar results were obtained when comparing Schemes 2 and 6 (from Fig. 2).

As Fig. 18 shows, the energy savings increases when the temperature of the heated furnace air increases, since the fraction of reuse air in mixture rises.

6. Conclusions

A mathematical model, algorithm and computer program for the simulation of cross flow driers with exhaust air recirculation, were developed. The iterative MacCormack's method with "time-split", which transformed the two-dimensional problem into a sequence of one-dimensional problems, was successfully applied for the solution of a system of non-linear partial differential equations. The simulations for the studied dryer outlines showed good performance of the developed program.

Non-uniformity of the temperature and moisture concentration fields in outlet cross-section of cross flow dryers depends strongly on the grain dryer outline and can be significant.

Reversing the airflow direction equalises the distribution of parameters in the transverse dryer direction. At the same time, the optimal reversal number is one or two (*i.e.* two or three stages). The influence of the increase of the air humidity due to reuse of air on the dryer performance can be neglected.

Upward motion of the reuse air from stage to stage, *i.e.* against the direction of motion of the grain mass, gives higher energy savings compared with downward motion.

For three-stage dryers, the use of the different initial air temperatures for different stages allows to obtain a more uniform distributions of temperature and moisture content, if to use the maximum temperature in the second stage and the minimum temperature in the third stage. For a two-stage dryer, the use of the same inlet air temperature in the both stages is preferred.

Validation of the software using experimental data for the full-scale dryers is required.

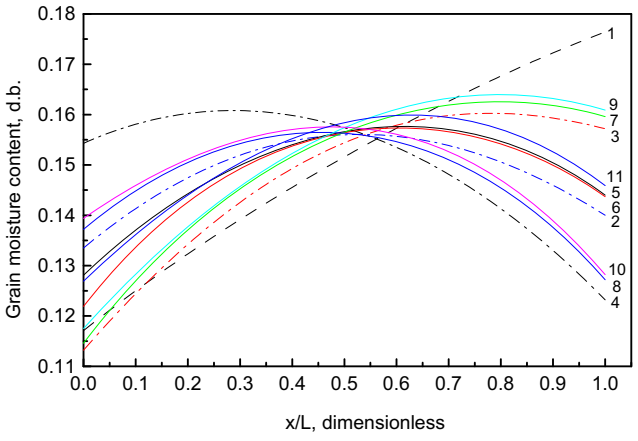

Fig. 8 – Grain moisture content distribution in outlet cross-section of studied dryers (curves number corresponds to the simulations in Table 1).

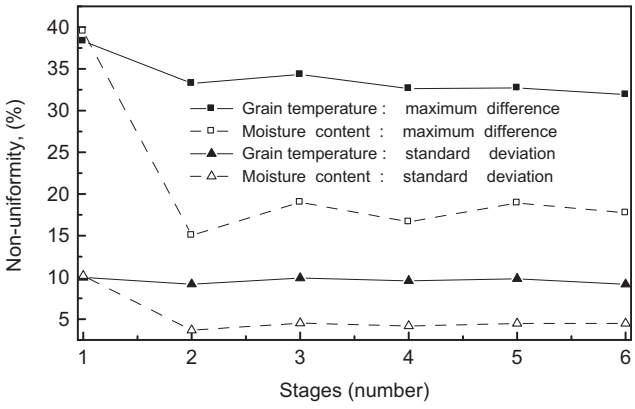

Fig. 9 – Influence of number of stages on the non-uniformity of grain temperature and moisture content in outlet cross-section of dryer (at the cooling entry).

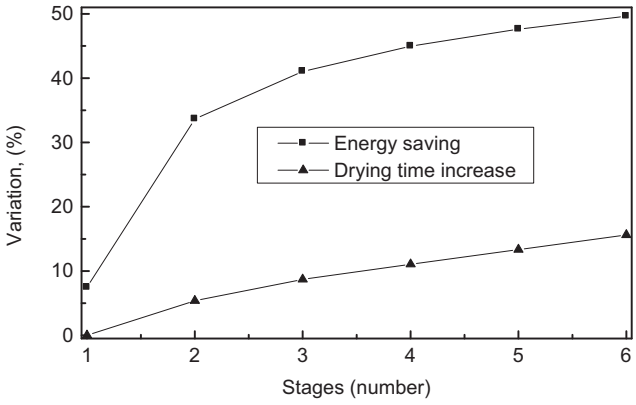

Fig. 10 – Influence of number of stages on energy saving and drying time.

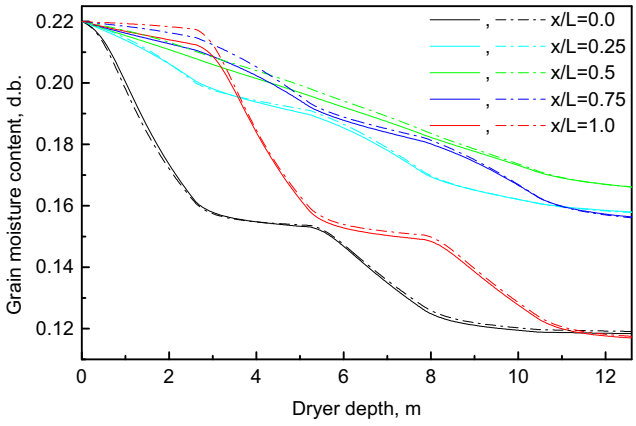

Fig. 11 – Influence of additional humidity caused by air reuse on drying in a four stage dryer (outline design 4 in Fig. 2); continuous line: without air reuse; dash dot line: with air reuse.

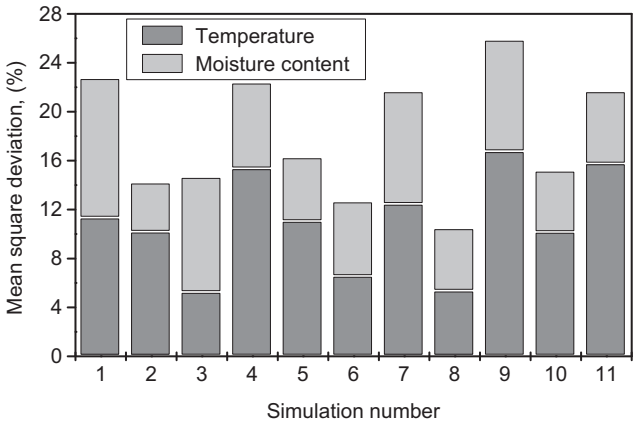

Fig. 12 – Mean square deviations of grain temperature and moisture content in outlet cross-section of studied dryers (simulation details in Table 1).

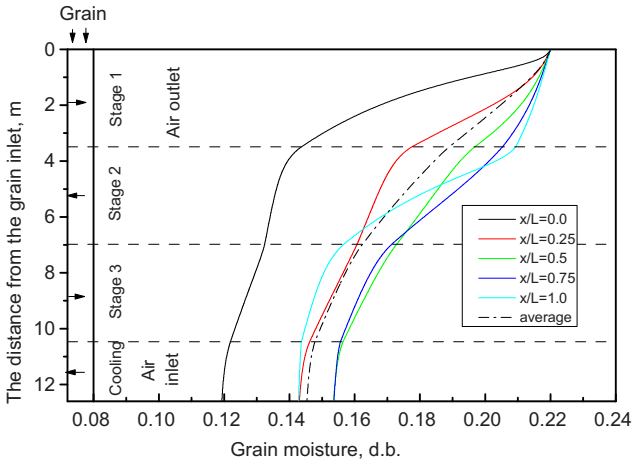

Fig. 13 – Distribution of moisture content of grain for the simulation 6 (Table 1) at a steady state.

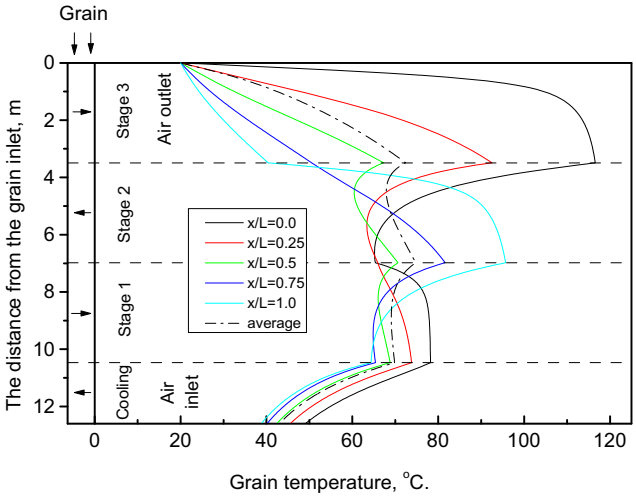

Fig. 14 – Distribution of grain temperature for the simulation 6 (Table 1) at a steady state.

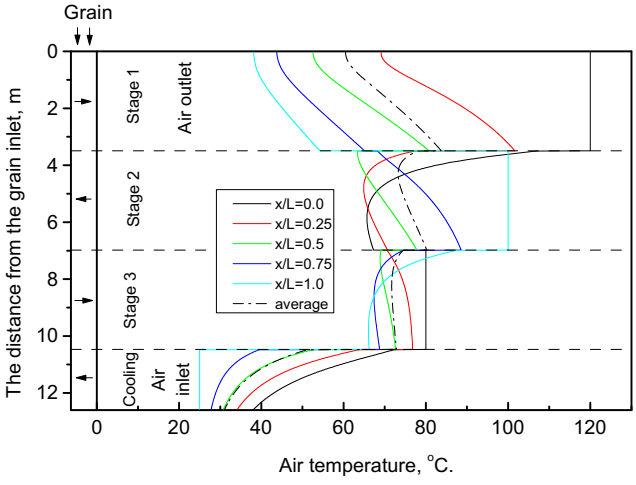

Fig. 15 – Distribution of air temperature for the simulation 6 (Table 1) at a steady state.

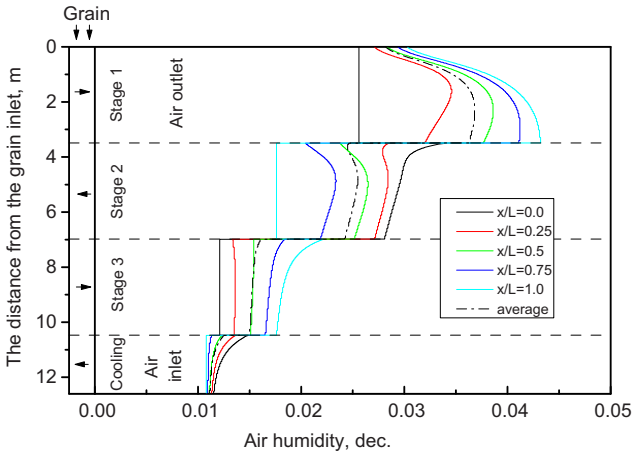

Fig. 16 – Distribution of air humidity for the simulation 6 (Table 1) at a steady state.

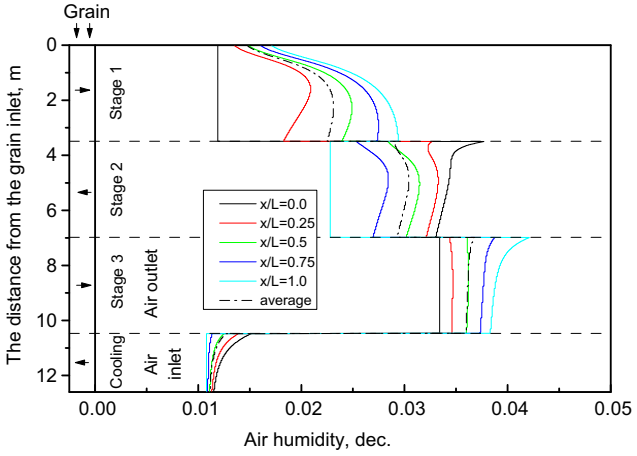

Fig. 17 – Distribution of air humidity for the outline design 5 (Fig. 2) at a steady state.

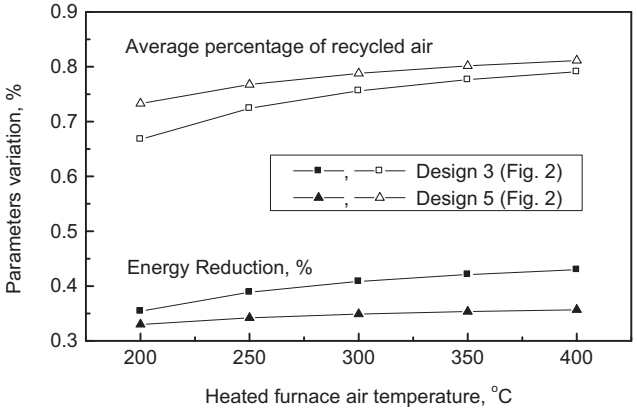

Fig. 18 – Influence of the temperature of heated furnace air on the energy reduction (solid points) and average percentage of recycled air (open points): square points, outline design 3; triangular points, outline design 5 (Fig. 2).

Acknowledgements

The first and second authors are grateful to CNPq for research grants (process N° 313706/2009-3 e N° 475237/2009-9).

REFERENCES

Barrozo, M. A. S., Felipe, C. A. S., Sartori, D. J. M., & Freire, J. T. (2006). Quality of soybean seeds undergoing moving bed drying: countercurrent and crosscurrent flows. *Drying Technology, 24*, 415–422.

Barrozo, M. A. S., Henrique, H. M., Sartori, D. J. M., & Freire, J. T. (1999). Drying of soybean seeds in a crossflow moving bed. *The Canadian Journal of Chemical Engineering, 77*, 1121–1126.

Brooker, D. B., Bakker-Arkema, F. W., & Hall, C. W. (1982). *Drying cereal grains*. Westport, CT: AVI Publishing Co.

Courant, R., Friedrichs, K., & Lewy, H. (1967). On the partial difference equations of mathematical physics. *IBM Journal of Research and Development, 11*, 215–234.

Courtois, F., Lebert, A., Lasseran, J. C., & Bimbenet, J. J. (1991). Simulation of industrial dryers: solving numerical and computer problems. *Drying Technology, 9*(4), 927–945.

Eltigani, A. Y., & Bakker-Arkema, F. W. (1987). Automatic control of commercial crossflow grain dryers. *Drying Technology, 5*(4), 561–575.

França, A. S., Fortes, M., & Haghighi, K. (1994). Numerical simulation of intermittent and continuous deep-bed drying of biological materials. *Drying Technology, 12*(7), 1537–1560.

Giner, S. A., Mascheroni, R. H., & Nellist, M. E. (1996). Cross-flow drying of wheat. A simulation program with a diffusion-based deep-bed model and a kinetic expression for viability loss estimations. *Drying Technology, 14*(7, 8), 1625–1672.

Han, F., Zuo, C. C., Zhu, H., Wu, W. F., & Liu, C. S. (2012). The establish of digital simulation system on continuous cross-flow dryer. *Advanced Materials Research, 430–432*, 1759–1763.

Jayas, D. S., Cenkowski, S., Pabis, S., & Muir, W. E. (1991). Review of thin-layer drying and wetting equations. *Drying Technology, 9*(3), 551–588.

Kemp, I. C. (1999). Progress in dryer selection techniques. *Drying Technology, 17*(7&8), 1667–1680.

Khatchatourian, O. A. (2012). Experimental study and mathematical model for soya bean drying in thin layer. *Biosystems Engineering, 113*(1), 54–64.

Khatchatourian, O. A., & Oliveira, F. A. de (2006). Mathematical modelling of airflow and thermal state in large aerated grain storage. *Biosystems Engineering, 95*(2), 159–169.

Laws, N., & Parry, J. L. (1983). Mathematical modeling of heat and mass transfer in agricultural grain drying. *Proceedings of the Royal Society of London, A385*, 169–187.

Liu, Q., & Bakker-Arkema, F. W. (2001). Automatic control of crossflow grain dryers, Part 1: development of a process model. *Journal of Agricultural Engineering Research, 80*(1), 81–86.

Luikov, A. V. (1966). *Heat and mass transfer capillary-porous bodies*. New York: Pergamon.

MacCormack, R. W. (1969). *The effect of viscosity in hypervelocity impact cratering*. AIAA Paper, 69–354, Cincinati, Ohie.

MacCormack, R. W. (1971). *Numerical solutions of the interaction of a shock wave with a laminar boundary layer*. In *Lecture notes in physics* (Vol. 8 (pp. 151–163). Springer-Verlag.

MacCormack, R. W., & Paullay, A. J. (1972). *Computational efficiency achieved by time splitting of finite difference operators*. AIAA Paper, 72–154, San Diego, California.

Marinos-Kouris, D., Maroulis, Z. B., & Kiranoudis, C. T. (1998). Modeling, simulation and design of convective industrial dryers. *Drying Technology, 16*(6), 993–1026.
Mayta, S. M. A., Massarani, G., & Pinto, J. C. (1996). Modeling of grain drying in continuous cross-flow sliding bed dryers. *Canadian Journal of Chemical Engineering, 74*, 797–805.
Moreira, R. G., & Bakker-Arkema, F. W. (1990). A feedforward/feedback adaptive controller for commercial cross-flow grain driers. *Journal of Agricultural Engineering Research, 45*, 107–116.
Parry, J. L. (1985). Mathematical modelling and computer simulation of heat and mass transfer in agricultural grain drying: a review. *Journal of Agricultural Engineering Research, 32*(1), 1–29.
Parti, M. (1993). Selection of mathematical models for drying grain in thin-layers. *Journal of Agricultural Engineering Research, 54*, 339–352.
Platt, D., Rumsey, T. R., & Palazoglu, A. (1991). Dynamics and control of cross-flow grain dryers. I. Model development and testing. *Drying Technology, 9*(1), 27–60.
Rumsey, T. R. (1986). *Transient simulation of a cross flow rice dryer*. ASAE, Paper No. 86-6906, St. Joseph, MI.
Rumsey, T. R., & Rovedo, C. O. (2001). Two-dimensional simulation model for dynamic cross-flow rice drying. *Chemical Engineering and Processing, 40*(4), 355–362.
Tórrez, N., Gustafsson, M., Schreil, A., & Martínez, J. (1998). Modeling and simulation of a crossflow moving bed grain dryers. *Drying Technology, 16*, 1999–2015.
Zhihuai, M., & Chongwen, C. (1999). Simulation and optimization of cross flow grain dryers. *Drying Technology, 17*(9), 1767–1777.